18

Self-Similarity in Semiconductors: Electronic and Optical Properties

L. M. Gaggero-Sager[1], E. Pujals[2], D. S. Díaz-Guerrero[1] and J. Escorcia-García[1]
[1]*Universidad Autónoma del Estado de Morelos*
[2]*Instituto de Matemática Pura e Aplicada - IMPA Brasil*
[1]*México*
[2]*Brasil*

1. Introduction

Since the first time the human reason glimpse at the subatomic world, the idea that an atom resembles the solar system appear very natural, although wrong. This idea have intrinsically the notion of self-similarity, i. e., the matter organizes in a very similar, but not the same, way at different scales of length. The self-similarity in nature has been considered and searched for by many scientists from different fields of knowledge. But perhaps the most accurate description, as usual, came from mathematics.
The middle third Cantor set $\mathcal{C}$ is one of the simplest examples of self-similarity and give us the opportunity of emphasize a key feature, self-similarity exist only in sets. So, a function would be self-similar if its image set is self-similar. Although $\mathcal{C}$ is self-similar it has other interesting properties, e. g., it is a perfect set, it is totally disconnected, and a very astonishing one is that it has the same cardinality as $\mathbb{R}$.
Finally it seems appropriate to mention that the study of irregular objects has a very important reason, the world around us is not made of lines, planes and spheres, at least not in the human eye scale. For this reason it is crucial to consider other type of "geometries". In this spirit the fractal geometry was very promising and visually very spectacular, but has some disadvantages, such as that the very definition of a fractal discard immediately every physical object. Nonetheless, it is worth to mention it because of the relation between fractals and self-similar sets. In the rest of this section we try to give a general overview about the concepts mentioned here as well as the formal definitions of the more relevant ones.

1.1 Self-similar sets

As mentioned before, self-similarity is a feature of sets and is more evident in its geometrical representation. So before giving the formal definitions, let us take a look at some illustrative examples.
The first thing that should be notice is the scale invariance of both figures, that is, if you take a part of the Sierpinski's triangle and zoom in, you should see the whole figure again. In the case of the Koch's snowflake, you don't get the whole snowflake when zoom in, instead you

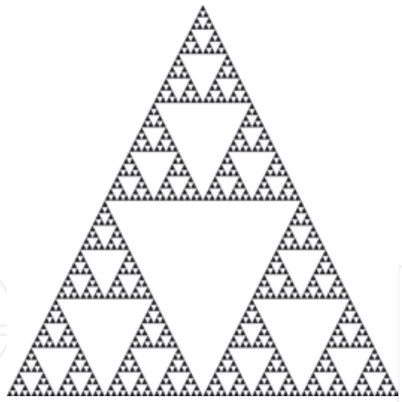

Fig. 1. Sierpinski's triangle.

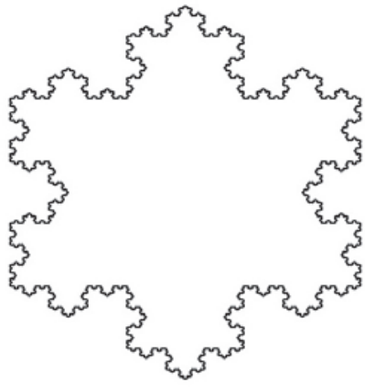

Fig. 2. Koch's snowflake.

get what is called the Koch's curve. This examples shows that the equivalence under scaling is not exact but similar. The case of the Cantor set is more simple and less visually exiting because it 'lives' in (is a subset of) the real line. However we will use the Cantor set in the coming sections so we should give a more detailed description of it, but before we translate this ideas into formal definitions that are more convenient to work with.

Definition A map $S : \mathbb{R}^d \to \mathbb{R}^d$ is a **similitude** with ratio $r > 0$ if $\forall x, y \in \mathbb{R}^d$

$$d(S(x), S(y)) = rd(x, y) \tag{1}$$

where $d : \mathbb{R}^d \to \mathbb{R}$ is a distance function. If $r \in (0, 1)$ S is called a contraction.

Definition A set $F \subset \mathbb{R}^d$ is called **self-similar** if given a family of similitudes $\{S_1, \ldots, S_n\}$ with the same ratio r

$$F = S_1(F) \cup \cdots \cup S_n(F) \tag{2}$$

Now we consider the most important example for our purposes, the Cantor's set. The traditional construction of this amazing set can be found in several books, and is based in the geometrical idea of removing the middle third open segment of the interval $[0, 1]$, which give us the first generation of the construction. Next, the process is repeated at infinitum for the remaining segments. What is left is the so called middle third Cantor's set $\mathcal{C}$. For our purposes

it seems more convenient to take the similitudes $S_1(x) := x/3$ and $S_2(x) := x/3 + 2/3$ with ratio $1/3$, and to build from them and the segment $\mathcal{C}_0 := [0,1]$. Let $\mathcal{C}_i := S_1(\mathcal{C}_{i-1}) \cup S_2(\mathcal{C}_{i-1})$ for $i = 1, 2, \ldots$. So, $\mathcal{C}_1 := S_1(\mathcal{C}_0) \cup S_2(\mathcal{C}_0)$ and $\mathcal{C}_2 := S_1(\mathcal{C}_1) \cup S_2(\mathcal{C}_1)$, etc. From this it is clear that

$$\mathcal{C}_2 = S_1(S_1(\mathcal{C}_0) \cup S_2(\mathcal{C}_0)) \cup S_2(S_1(\mathcal{C}_0) \cup S_2(\mathcal{C}_0)) \tag{3}$$

$$= (S_1 \circ S_1)(\mathcal{C}_0) \cup (S_1 \circ S_2)(\mathcal{C}_0) \cup (S_2 \circ S_1)(\mathcal{C}_0) \cup (S_2 \circ S_2)(\mathcal{C}_0) \tag{4}$$

Now denoting $S_i \circ S_j$ as S_{ij} and in a natural way $S_{i_1} \circ \cdots \circ S_{i_n}$ as $S_{i_1,\ldots,i_n}$ where $i_l = 1, 2$ we could write

$$\mathcal{C}_k = \bigcup_{\pi(i_1,\ldots,i_k)} S_{i_1,\ldots,i_k}(\mathcal{C}_0) \tag{5}$$

The union runs over all the possible sequences $i_1, \ldots, i_k$. So we get that

$$\lim_{k\to\infty} \mathcal{C}_k = \mathcal{C}. \tag{6}$$

This is similar to take the set $\mathcal{C} = Closure(\cap_k \mathcal{C}_k)$.

Quasiperiodic or quasiregular heterostructures (henceforth QH) follow an algorithmic sequence based on some self-replicating rule, for example the Fibonacci sequence among others. There is a great deal of current work on QH (see for example Refs. (1; 2)) and numerous references can be found in two recent reviews.(3; 4) In these kind of systems, the question of self-similarity was deeply examined but found to have a very limited range of validity in actual practice(5). In addition, the fractal character (6) of the spectrum of elementary excitations is rigorously proved (7; 8) and confirmed in many numerical calculations (see for example Refs. (3; 5)).

We propose the study of very different systems, inspired by QH and other self-similar systems. In particular, we aim to study semiconductor quantum systems in which the potential is close to a self-similar function (6) defined in a bounded interval. We hope this can be generalized and applied to other problems.

The study of this kind of potentials is motivated by the evidences that the transmittance reflects the self-similar property of the potential through its fractal dimension. In the other hand Lavrinenko et al (10; 11) studied the propagation of classical waves of the optical Cantor filter. This system is not a self-similar system, because the refractive indices are not scaled. The authors observed that the optical spectra has shown spectral scalability. In the last few years, a lot of experimental works concerning the worth noting properties of porous silicon in chemical and biological sensing have been reported (12). Moretti et al have compared the sensitivities of resonant optical biochemical sensor, based on both periodic and aperiodic porous silicon structures, such as Bragg and the Thue-Morse multilayer. They observed that the aperiodic multilayer is more sensitive than the periodic one. Finding other similar systems with larger sensitiveness would be important for applications.

Agarwal et al (13) have reported experimental results on electromagnetic wave propagation in nanostructures porous silicon multilayer where geometrical length follows the Cantor code. For generations higher than six equidistant fringes are observed instead photonic bands. Esaki et al (14)observed that for specific values of wave numbers, transmission coefficients are shown to be governed by the logistic map and, in the chaotic region, they show sensitive dependence on small changes in parameters of the system such as the index of refraction. In

the other hand, Pilevary Salmasi (15) et al studied a fractal shaped antenna using multilayer structure.
A significant number of papers have been also devoted to different mathematical aspects of this problem. See, for example, Refs. (16)-(17), and references therein.
The study of properties material's is due to the research on optimal devices with the goal to improve the present ones. With this in mind, and for methodological purposes, scientists look at the fundamental physical properties of such materials. One of the possibilities is the transmission coefficient, or transmittance, of an electromagnetic wave incident upon a quantum potential, typically barriers or wells. This topic is covered in the college courses for a single rectangular barrier, nevertheless is very interesting to study some more complex systems. Among these, there is the so called superlattices for which the transmittance has been well characterized by their band structure. An even more irregular case is the Cantor-like potential (1; 3), which is inspired in the Cantor set, in this system the height, widht and distance of the barriers (or wells) are modified just like int the construction of the Cantor set.

2. Topological self-similar quantum wells

In this section, first we are goint to introduce the selfsimilar quantum wells; later we show how the selfsimilarity are reflected in terms of the solution of the SchrÃűdinger's equation. This is done formally in subsection 2.2 and in subsection 2.3 from the point of view of semiclassical approximation. In subsection 2.4 we analyze numerical the properties of the discrete spectrum.

2.1 Definition and properties of the potential

Let us define the intervals $I = [0,1]$ and $J = [a,b]$, with $0 < a < b < 1$. Let us consider two differentiable functions $f_0 : [0,1] \to [0,a]$ and $f_1 : [0,1] \to [b,1]$, such that both are onto and $0 < |f_0'(x)| < \lambda_0 < 1$, $0 < |f_0'(x)| < \lambda_1 < 1$ for any $x \in [0,1]$. Given $a_N = (i_1, i_2, \cdots, i_N)$ an N-couple of 0's and 1's, i.e. $i_j = 0,1$ for all $j = 1,2,\cdots,N$, we define the composition functions

$$f_{a_N}(x) = f_{i_N} \circ \cdots \circ f_{i_2} \circ f_{i_1}(x)$$

and the intervals

$$I_{a_N} = f_{i_N} \circ \cdots \circ f_{i_2} \circ f_{i_1}(I_0) \tag{7}$$
$$J_{a_N} = f_{i_N} \circ \cdots \circ f_{i_2} \circ f_{i_1}(J_0). \tag{8}$$

We consider the particular case that the functions f_0, f_1 are affine; i.e. $\lambda_0 := |f_0'| = \frac{1}{a}$ and $\lambda_1 := |f_1'| = \frac{1}{1-b}$. Observe that the intervals I_{a_N} has length $\lambda_0^{a_N^0}\lambda_1^{N-a_N^0}$ where a_N^0 is the number of 0's that appear in the sequence a_N. In the same way, the intervals J_{a_N} has length $\lambda_0^{a_N^0}\lambda_1^{N-a_N^0}(b-a)$. To avoid notation, we denote $\lambda_{a_N} := \lambda_0^{a_N^0}\lambda_1^{N-a_N^0}$.
An special case of the above defined affine maps are the ones associated to the classical $1/3-$middle Cantor set where $f_0(x) = \frac{1}{3}x$ and $f_1(x) = \frac{1}{3}x + \frac{2}{3}$. In this situation, the intervals and functions just defined have a direct interpretation in terms of the standard Cantor construction. See Fig. 3. $I = [0,1]$ is the starting interval and $J = [1/3, 2/3]$ is the central one third interval of I.

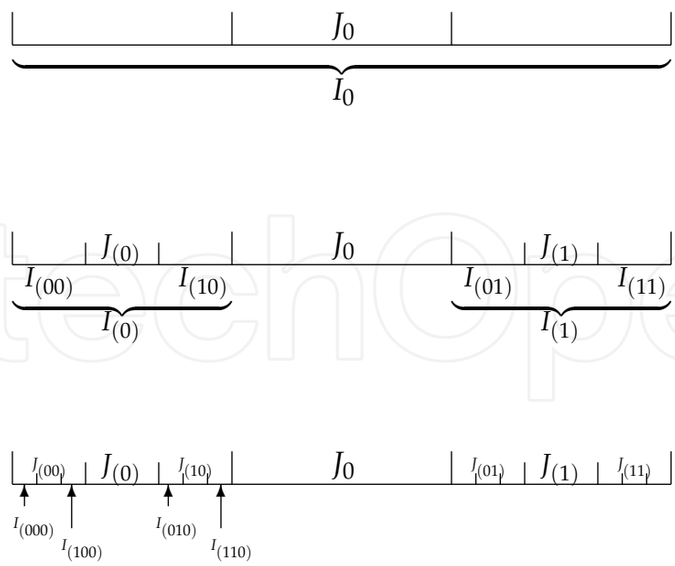

Fig. 3. The three first generations of Cantor construction. For the sake of clarity the starting interval I_0 is only denoted in the upper panel, and intervals $I_{(0)}$ and $I_{(1)}$ are only denoted in the middle panel.

For more general and precise construction of cantor's map and the role that they played in theory of dynamical systems see (18; 19).

Now, we take $0 < \alpha_0 < 1$ and $0 < \alpha_1 < 1$ and we denote $\alpha_{a_N} := \alpha_0^{a_N^0} \alpha_1^{N-a_N^0}$. From that, we define the potential equal to $V_0 \alpha_{a_N}$ in any of the intervals J_{a_N} and zero elsewhere. V_0 is some amplitude irrelevant for the following.

Observe that this potential verifies the following property that resembles the classical notion of self-similarity:

$$V(f_{a_N}^{-1}(x)) = \frac{1}{\alpha_{a_N}} V(x) \quad \forall\, x \in f_{a_N}(I_0)\ . \tag{9}$$

Indeed, this condition would be a full self-similarity if it is fulfilled for all values of the coordinate variable x. Since it only holds for x in certain intervals, the arguments in the spirit of Group Theory can not be pursued. However, in the following we call this condition *self-similarity*, or in any case *quasi-self-similarity*, due to the close resemblance with the theoretical pure situation of self-similarity.

2.2 Formal solution and self-similarity

We will now explain, in a little more rigorous and general manner, a theorem regarding the self-similarity of the wave functions of the continuous spectrum when the potential is a self-similar function.

Let $E > 0$, $k > 0$ ($k = \hbar^2/(2m(x))$ where $m(x)$ is the position-dependent effective mass). In the sequel, we will note with $\Psi_{E,k}$, the solution of the problem

$$k\Psi_{E,k}(x) + (E - V(x))\Psi_{E,k}(x) = 0 \tag{10}$$

We want to study how the self-similarity of the potential $V(x)$ -and the mass $m(x)$- is reflected in the eigenfunctions and eigenvalues. More precisely we want to see if there exist some similarity between the eigenfunction restricted to the whole interval, and the same (or another) eigenfunction, when it is restricted to the interval $f_{a_N}(I_0)$. In others words, we want to see, if given E and $k > 0$, there exist $E' > 0$ and $k' > 0$ such that

$$\Psi_{E,k}(f_{a_N}^{-1}(x)) = \Psi_{E',k'}(x) \tag{11}$$

for any $x \in f_{a_N}(I_0)$. In this direction, we obtain the following Theorem which is a renormalization Theorem.

Theorem 1. *Let $E > 0$, $k > 0$ and the eigenfunction $\Psi_{E,k}$. Given $N > 0$ then we get that*

$$\Psi_{E,k}(f_{a_N}^{-1}(x)) = \Psi_{E',k'}(x)$$

for any $x \in f_{a_N}(I)$, where $E' = E\alpha_{a_N}, k' = \lambda_{a_N}^2 \alpha_{a_N} k$

Before to give the proof, observe that the Theorem is showing equivalently, that given $N > 0$ then

$$\Psi_{E,k}(f_{a_N}(x)) = \Psi_{E',k'}(x)$$

for any $x \in I$.
Now, let us give the proof.
Proof: We have that

$$k\Psi''_{E,k}(x) + (E - V(x))\Psi_{E,k}(x) = 0 \tag{12}$$

with $x \in [0, 1]$.
Taking the transformation $f_{a_N}^{-1} : f_{a_N}(I) \to I$, we get that for any $x \in f_{a_N}(I)$

$$k\Psi''_{E,k} \circ f_{a_N}^{-1}(x) + (E - V \circ f_{a_N}^{-1}(x))\Psi_{E,k} \circ f_{a_N}^{-1}(x) = 0\,. \tag{13}$$

Using that $\Psi''_{E,k} \circ f_{a_N}^{-1} = \lambda_{a_N}^2 (\Psi_{E,k} \circ f_{a_N}^{-1})''(x)$ and that $V(f_{a_N}^{-1}(x)) = \frac{1}{\alpha_{a_N}} V(x)$,

$$\lambda_{a_N}^2 k(\Psi_{E,k} \circ f_{a_N}^{-1})''(x) + (E - \frac{1}{\alpha_{a_N}} V(x))\Psi_{E,k} \circ f_{a_N}^{-1}(x) = 0 \tag{14}$$

for any $x \in f_{a_N}(I)$ and equivalently,

$$\alpha_{a_N} \lambda_{a_N}^2 k(\Psi_{E,k} \circ f_{a_N}^{-1})''(x) + (\alpha_{a_N} E - V(x))\Psi_{E,k} \circ f_{a_N}^{-1}(x) = 0 \tag{15}$$

for any $x \in f_{a_N}(I)$. This implies that $\Psi_{E,k} \circ f_{a_N}^{-1}$ is solution of

$$k' Y''(x) + (E' - V(x))Y(x) = 0\,, \tag{16}$$

where $k' = \lambda_{a_N}^2 \alpha_{a_N} k$, and $E' = E\alpha_{a_N}$. And this means that

$$\Psi_{E,k}(f_{a_N}^{-1}(x)) = \Psi_{E',k'}(x) \tag{17}$$

for $x \in f_{a_N}(I)$. This finishes the proof.

2.3 Semiclassical solution and self-similarity

Observe that in the particular case of the standard 1/3 Cantor set for the potential defined above the following properties are satisfied.

$$\text{if } 0 \leq x \leq 1/3 \quad \text{then} \quad V(x) = \frac{1}{3}V(3x) \tag{18}$$

$$\text{if } \frac{2}{3} \leq x \leq 1 \quad \text{then} \quad V(x) = \frac{1}{3}V(3x-2)\ . \tag{19}$$

Now, let $E > \text{Max}[V(x)]$, be a eigenvalue of the continuous spectrum of the Schrödinger equation:

$$\frac{d^2F(x)}{dx^2} + \frac{2m}{\hbar}(E - V(x))\ F(x) = 0\ . \tag{20}$$

For this eigenvalue, using semiclassical approximation, we get that the associated eigenfunction is (20)

$$F_E(x) = A_E(x)\ \exp\left[\frac{i}{\hbar}\ S_E(x)\right] \tag{21}$$

where

$$A_E(x) = \frac{C_1}{(2m\,(E - V(x)))^{1/4}} \tag{22}$$

$$S_E(x) = \int_0^x \sqrt{2m(E - V(x))}\ \ dx\ . \tag{23}$$

Using the properties of $V(x)$, observe that for any $x \in [0, 1/3]$

$$\begin{aligned} A_E(x) &= \frac{C_1}{(2m(E - V(x)))^{1/4}} = \frac{C_1}{(2m(E - \frac{1}{3}V(3x))^{1/4}} \\ &= 3^{1/4}C_1 A_{3E}(3x)\ . \end{aligned} \tag{24}$$

This means that, up to a certain constant, the function A_E (of the eigenvalue E) in the interval $0 \leq x \leq 1/3$ is equal to the function A_{3E} (of the eigenvalue $3E$) in the interval $0 \leq x \leq 1$. On the other hand, for the function S_E, we have that for $x \in [0, 1/3]$

$$S_E = \frac{1}{\hbar}\int_0^x \sqrt{2m\left(E - \frac{1}{3}V\,(3x)\right)}\ \ dx\ . \tag{25}$$

Changing the integration variable x by $x' = 3x$, we have that for $x \in [0, 1/3]$

$$S_E(x) = \left(\frac{1}{3}\right)^{3/2} \int_0^{3x} \sqrt{2m\left(3E - V\left(x'\right)\right)}\ dx'$$
$$= \left(\frac{1}{3}\right)^{3/2} S_{3E}(3x)\ . \tag{26}$$

So, for $x \in [0, 1/3]$

$$F_E(x) = C_1 \left(\frac{1}{3}\right)^{1/4} A_{3E}(3x) \cdot$$
$$\cdot \exp\left[\frac{i}{\hbar}\left(\frac{1}{3}\right)^{3/2} S_{3E}(3x)\right]\ . \tag{27}$$

That is, the eigenfunction corresponding to the state E in the interval $\left[0, \frac{1}{3}\right]$ is self-similar to the eigenfunction corresponding to the state $3E$ in the interval $[0, 1]$. Arguing in the same way, and using the self-similarity of the potential in $\left[\frac{2}{3}, 1\right]$ we conclude also that the eigenfunction corresponding to the state E in the interval $\left[\frac{2}{3}, 1\right]$ is self-similar to the eigenfunction corresponding to the state $3E$ in the interval $[0, 1]$. Again, arguing in the same way we get that for any interval $f_{a_N}(I_0)$ (see previous section for definitions) the semiclassical approximation associated to the eigenvalue E over the interval $f_{a_N}(I_0)$ is self-similar over the interval $[0, 1]$ to the semiclassical approximation associated to the eigenvalue $3^N E$.
Since any value of E is an eigenvalue of the Schrödinger equation, then the self-similarity of the wave function is fulfilled for any value of E. This implies that for a quantum well with self-similar potential, it affects the wave functions in the whole continuous spectrum, not only the wave functions of the eigenvalues close to the well's limits, as would happen in a normal quantum well. This conclusion is general for any self-similar potential.

2.4 The case of the discrete spectrum

However, our interest is focused on electronic properties. So, we have to look to the discrete levels. For wave functions in discrete levels, it is impossible to find a general formula like those developed in previous sections in the framework of WKB Approximation. So we focus our attention on the resolution of a concrete problem using transfer matrix method (see for example (21) and references therein). Due to the fact that in semiconductors it is possible to grow potentials of different types, we propose the calculation of the discrete levels of the potential given in figure 4, constructed in AlGaAs/GaAs. We calculate the eigenvalues and eigenfunctions of this system in the Envelope Function Approximation (EFA)(22) with an effective mass of 0.068 m_0, where m_0 is the free electron mass and the well width is 6000 Å.
Let us consider a quantum well in AlGaAs/GaAs with a 1/3 Cantor-like shape [3] with rigid walls at the ends as shown in figure (1).
We calculate the eigenvalues and eigenfunctions of this system in the Envelope Function Approximation (EFA) with a effective mass of $0.068m_0$, where m_0 is the mass of the free electron,the dielectric constant being $\epsilon_r = 12.5$ and the well width of 6000 Å.

Let $\Psi(z)$ be a column vector with two components,

$$\Psi(z) = \begin{pmatrix} F(z) \\ F^{'}(z) \end{pmatrix}$$

and the matrix $P(z)$,

$$P(z) = \begin{pmatrix} 0 & 1 \\ -2m^* / \hbar^2 [E - V(z)] & 0 \end{pmatrix}$$

Thus

$$P(z)\ \Psi(z) = 0$$

Let $g_1(z)$ and $g_2(z)$ be two linearly independent solutions of the Schrödinger equation, then, from the transfer matrix formalism let us take

$$M(z, z_0) = \frac{1}{\Delta} \begin{pmatrix} g_2'(z_0)g_1(z) - g_1'(z_0)g_2(z) & g_1(z_0)g_2(z) - g_2(z_0)g_1(z) \\ g_2'(z_0)g_1'(z) - g_1'(z_0)g_2'(z) & g_1(z_0)g_2'(z) - g_2(z_0)g_1'(z) \end{pmatrix}$$

where

$$\Delta = g_1(z_0)g_2'(z_0) - g_1'(z_0)g_2(z_0)$$

and

$$\Psi(z) = M(z, z_0)\Psi(z_0)$$

Our potential is sectionally constant in all intervals. If we use the trigonometric functions, we obtain the exact result. For the calculation of the eigenvalues we use the boundary conditions, i.e., our potential is infinite in $z = l_{qw}$ and $z = -l_{qw}$, the transcendental equation by calculation of eigenvalues is $M_{12}(0, -l_{qw}) = 0$, for odd states and $M_{22}(0, -l_{qw}) = 0$ for even states, where M_{ij} are the elements ij of the matrix $M(l_{qw}, -l_{qw})$. Once we have the eigenvalues, the eigenfunctions are calculated in the usual manner, using the transference matrix method [5].

This system is actually a set of coupled quantum wells, therefore, we expect to observe self-similarity for basic states corresponding different wells as for excited states. Even if we did not observe the same structure of self-similarity as the one obtained for continuous spectrum, we do observe some interesting properties in the states of the discrete spectrum. For example, the states $E_1 = 1.104$ meV, $E_{46} = 361.9$ meV, and $E_{58} = 490.7$ meV are self-similar among themselves. In fact, the three states correspond to the basic levels of the different wells. The same thing happens with the first and second excited levels. In figure 5 (top panel) and 5 (bottom panel) the states $E_{17} = 135.4$ meV and $E_{49} = 397.0$ meV are observed, which are self-similar and this self-similarity does not respond to the simple coupling between wells. In figure 6 we present the state $E_{62} = 510.0$ meV, which is self-similar to itself. This occurs whether they are either self-similar or some kind of renormalization property between different states hold. On the other hand, we have observed that the density of the localized charge (the product of the eigenvalue with the eigenfunction) presents self-similarity (9).

2.5 Intersubband optical absorption

In Fig. 7 we depict the absorption coefficient due to intersubband transitions as a function of photon energy. The calculation method can be found in many textbooks. See, for example Ref. (22). As expected, the graphics is a sectionally constant function, and consequently, its derivative is a set of delta function peaks. Theoretical and numerical methods tend to

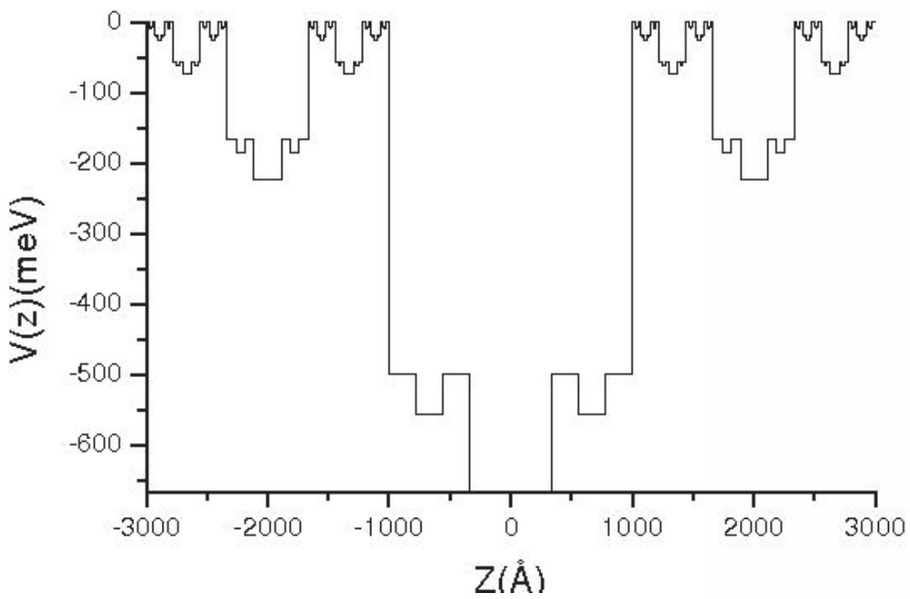

Fig. 4. Self-similar potential profile constructed as a fifth order Cantor function. This potential is scaled by three.

smooth this kind of graphics; this indicates the convenience of using the derivatives instead the original function in order to find the shoulders of the absorption coefficient as a function of energy. The calculation of fractal dimensions $D(q)$ of this set produces a value of 1 for q negative or about zero and a value neatly below 0.6 for q greater than 5. Then, the fractality of the spectrum has been transferred to the absorption coefficient.

3. GaAs-AlGaAs like heterostructure

To perform the calculations we used the parameters of the GaAs already mentioned. Assuming parabolic bands, in the low temperature limit, the charge density of the i^{th} level, is given by:

$$\rho_i(z) = \sum_{j=1}^{i} \left| F_j(z) \right|^2 E_j$$

where the $F_j(z)$ and E_j are the eigenfunctions and eigenvalues of the potential presented in Fig.1

In Fig.2 the charge density of the i^{th} level of the proposed system is presented for the first 100 energy levels. The self-similarity is evident. Then as it can be seen, self-similarity is not an exclusive property of infinite systems. Here we have shown that a self-similar finite quantum system may also exhibit self-similarity. In this case, self-similarity is evident in the charge density and this is a physically clear result. Other physically relevant parameters could in principle exhibit fractal characteristics in finite systems.

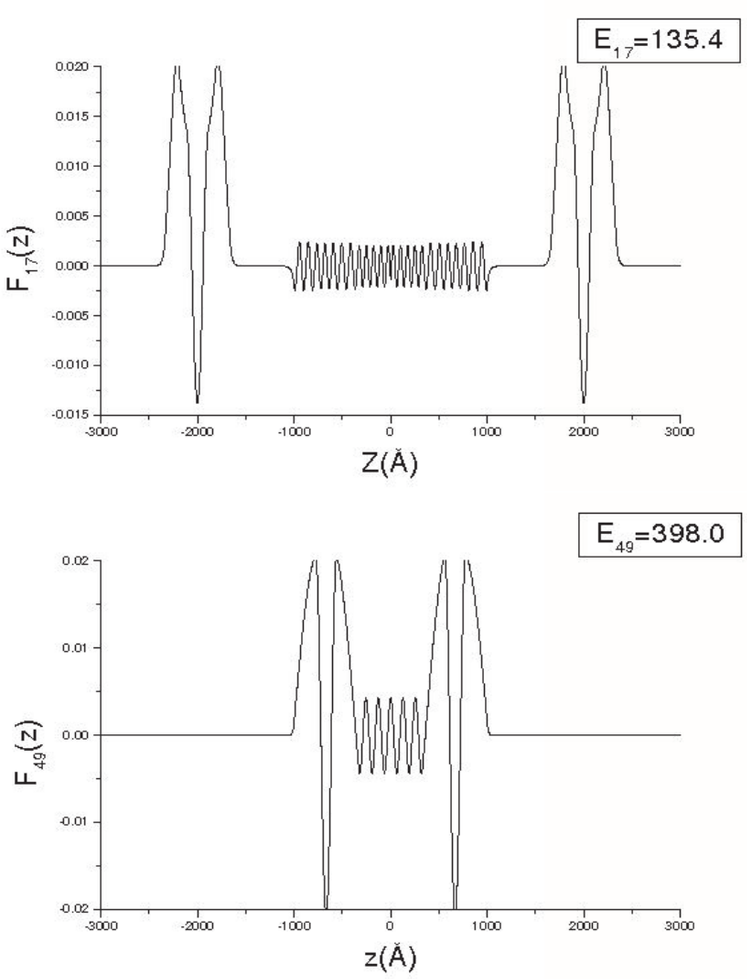

Fig. 5. Top panel: Eigenfunction corresponding to the eigenvalue $E_{17} = 135.4$ meV. Bottom panel: Eigenfunction corresponding to the eigenvalue $E_{49} = 397.0$ meV.

4. Self-similar barrier systems

4.1 Introduction

In this section we present the important case of strict self-similar potentials and their electronic transmission coefficient. This potentials are constructed based on the the construction of the Cantor set, i. e., are based on an iterated replacement of the zero potential zones by scaled copies of the main barrier, figure 10.

The set of parameters of this kind of systems are the follows: the value of the main barrier $H0$, the total length of the multibarrier system and the generation of the potential. Let us take a look at the transmission coefficient corresponding to the eighth generation of the self-similar potential with $H0 = 500meV$ and length from $Lt = 75$Åto $Lt = 750$Å, figure 11.

This shows that the total length determine the oscillatory behavior of the transmission coefficient, so, if we take this potential isolated, we must focus in lengths grater than 200Åin order to obtain some oscillations in our transmission curves.

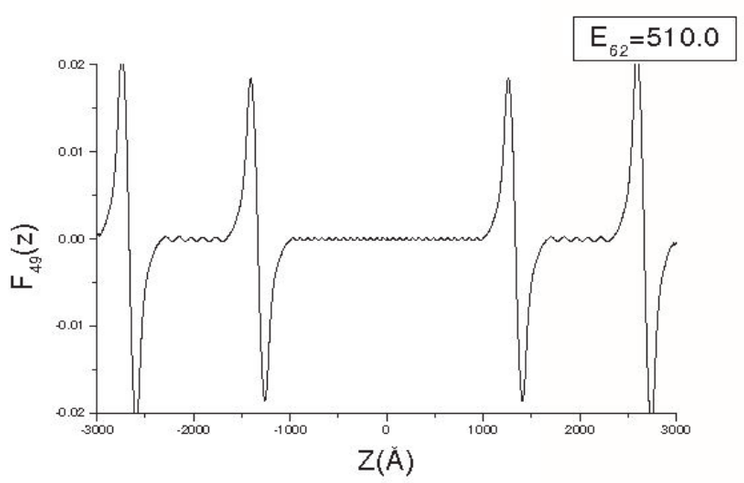

Fig. 6. Eigenfunction corresponding to the eigenvalue $E_{62} = 510.0$ meV.

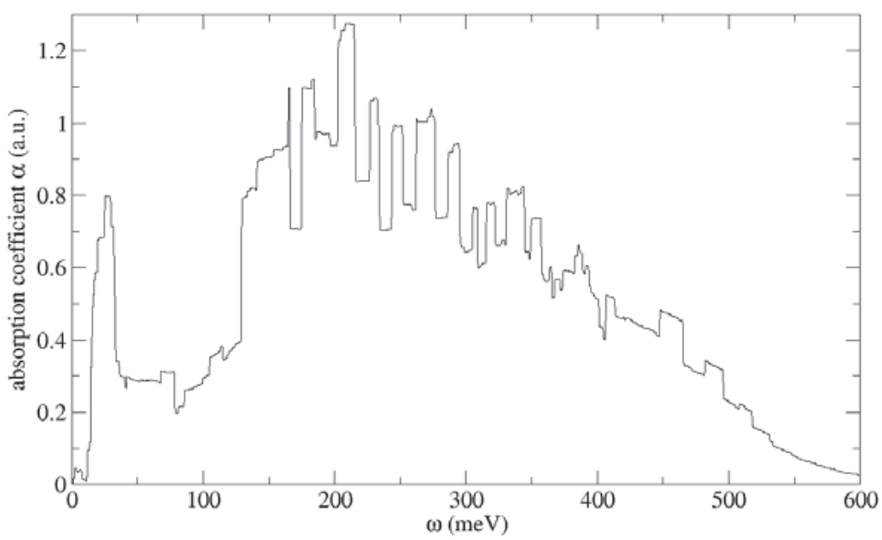

Fig. 7. Intersubband optical absorption coefficient.

It is also important to see what happens when we move from one generation of the potential to the next, in order to determine the effect, if any, of the self-similarity on the transmission coefficient. So in figure 12, we see the transmission coefficient curves for the first four generations of the self-similar potential.
Those curves could suggest that the self-similarity does not make much difference in the transmission coefficient, nevertheless, in the following subsection we will see that it's real contribution is really clear when is "mixed" with another type of structures.

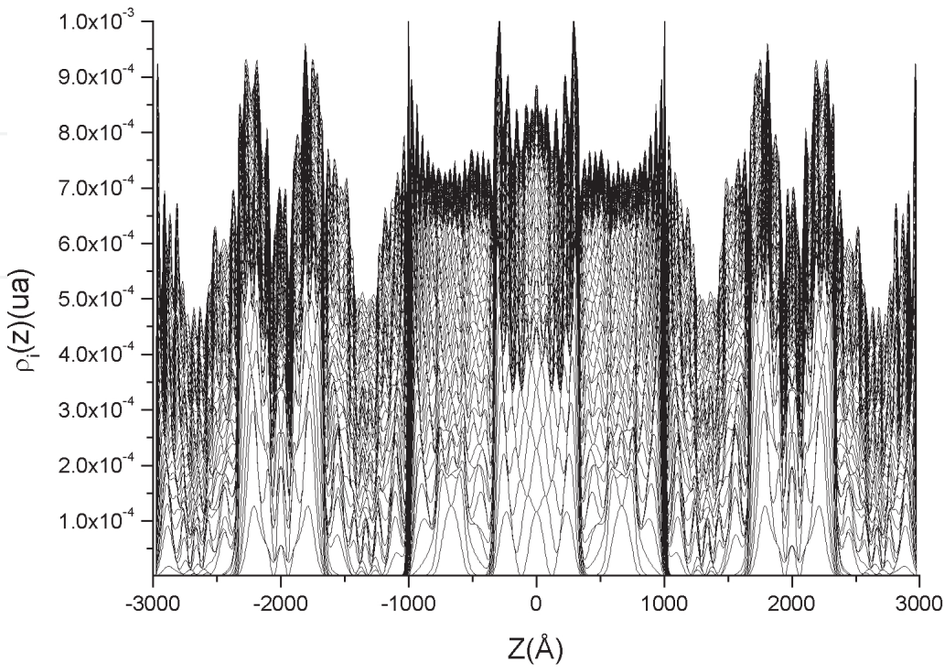

Fig. 8. Charge density.

4.2 Mixed multibarrier potentials

Now we consider a multibarrier system that mix the self-similar potential (henceforth ssp), and a multibarrier periodic potential (henceforth mbpp).

4.2.1 Methodology

An mixed multibarrier potential is built using two mbpp and one ssp. The mixing process is quite simple, in fact it is just an arrangement of the two systems in the following order, first a mbpp, next the ssp and then the other mbpp, see figure 13. It is important to notice that when the generation of the self-similar potential is increased the number of layers in the mbpp is increased linearly. The transfer matrix method is used to calculate the transmittance of the previous systems. These calculations are made in the framework of effective mass theory. In this system a given generation comprehend the same generation for the component systems, i. e., consider the generation three of the mixed multibarrier potential , it has two mbpp of three barriers each and one ssp of the third generation.

It is clear that the generation one corresponds to an mbpp of generation 3 (three layers), which most have the characteristic band structure. The parameters involved in this system are the height and width of the barriers and the distance between them. The parameters that are changed to study its effect on the transmittance are the width and distance. This parameter variation is applied to the mbpp systems. The key parameter for the ssp is the length of the whole structure, in this case 750Å. In figure 14 we present the transmittance for the mixed system. The first thing that one can note is the appearance of transmission peaks in the region between 250 and 350 meV, that seems to correspond to quasibound states for energies above

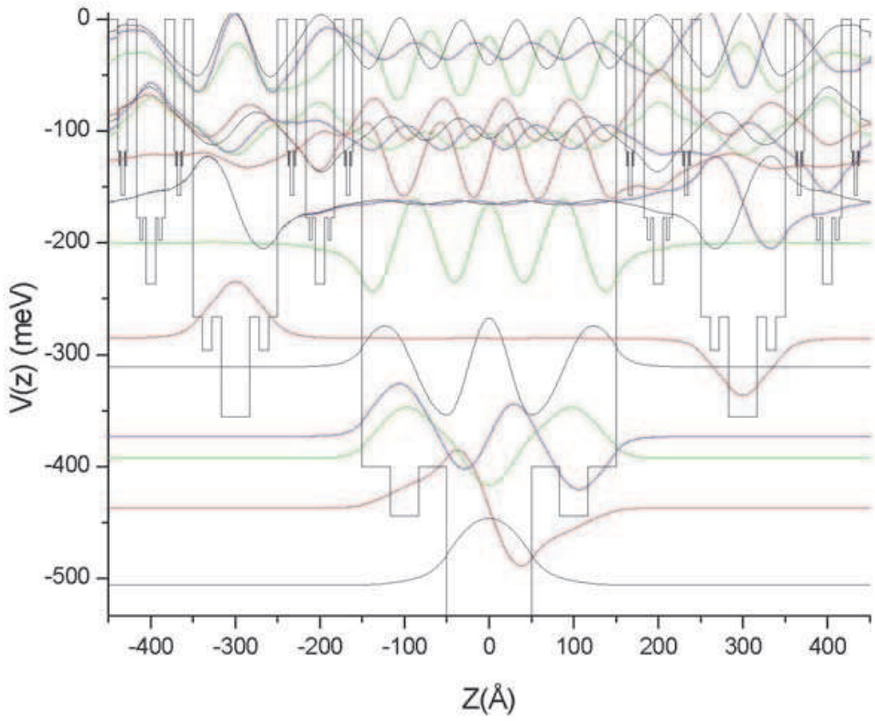

Fig. 9. Potential, energy levels and wave functions with scaling factor for the potential 3/2.

the value of V for the barriers. Those peaks are placed in the region corresponding to a gap in the mbpp. Finally it is worth to remark the following: it seems that those peaks are equidistant; the addition of the ssp to de mbpp rules out the tunneling region and the gaps in the transmittance are better defined.
Figure 15 shows that the inclusion of the ssp effectively made the tunneling band to disappear. Also, it shows quasibound states in energetic regions corresponding to gaps in the mbpp. Last but not least, it seems that the perfect reflection is obtained for the minimums of the gaps.

5. Optical case

5.1 Electromagnetic waves in self-similar multilayer systems

First we generalize the theorem 1 to the case of electromagnetic waves, so in the following we will use the construction of the potential given in section 2.1.

Theorem 2. *Let $N > 0$, $\omega > 0$ and $\boldsymbol{E}(x)$ the frequency and the electric field respectively. Then if $\boldsymbol{E}(x)$ is solution of then equation*

$$E''(x) - \frac{\omega^2}{v(x)^2} E(x) = 0 \tag{28}$$

we get that $E_\omega(f_{a_N}^{-1}(x)) = E_{\omega'}(x)$

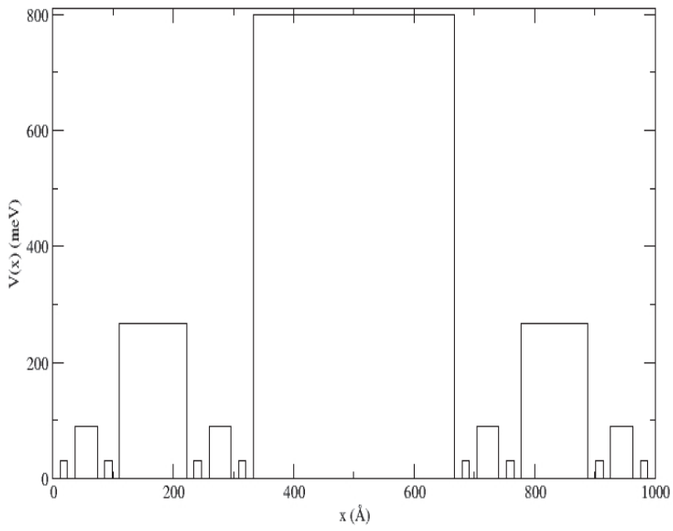

Fig. 10. Strict self-similar potential.

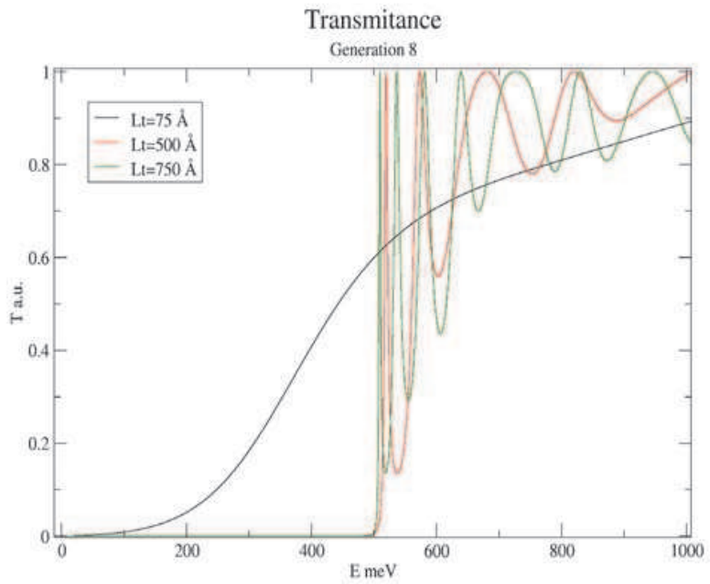

Fig. 11. Comparison of the transmission for the eighth generation of the GP-potential variyng the total length of the system.

Proof: First we take $\mathbf{E}(x,t) = E(x)e^{i\omega t}$, which give us the time-independent electric field equation Following the procedure for the quantum case, we consider the effect of the

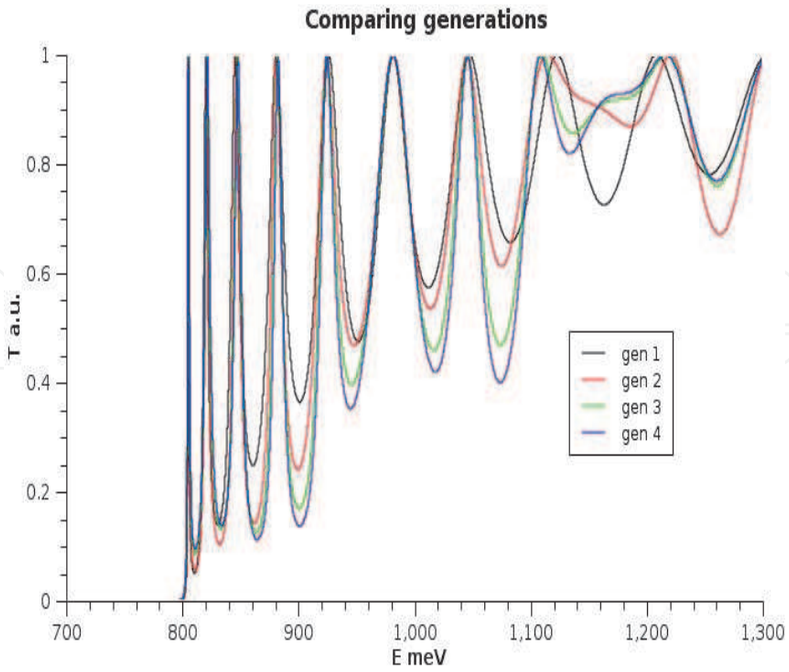

Fig. 12. Comparison of the first four generations of the GP-potential with $H0 = 800$ meV and $Lt = 1000$Å (total length).

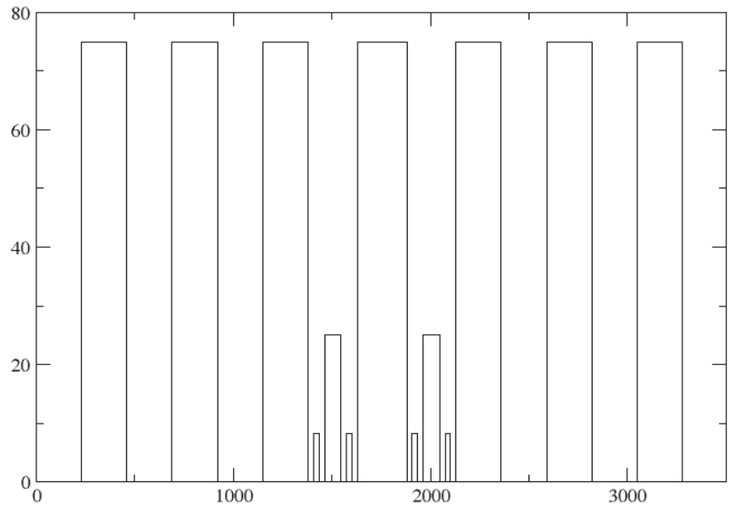

Fig. 13. Mixed Cantor-like potential, generation 3.

transformation $f_{a_N}^{-1}$ for the preceding equation

$$E'' \circ f_{a_N}^{-1}(x) - \frac{\omega^2}{v(x)^2} E \circ f_{a_N}^{-1} = 0 \tag{29}$$

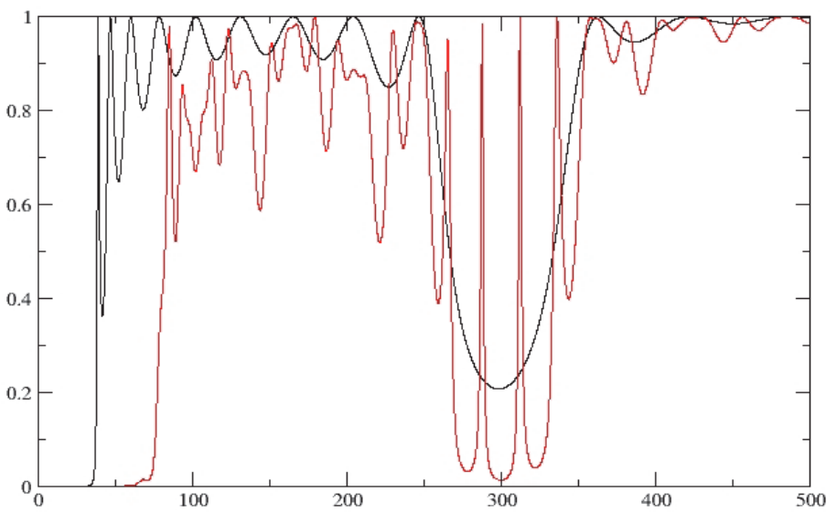

Fig. 14. Transmittance for an width/distance of 23Å, generation 10.

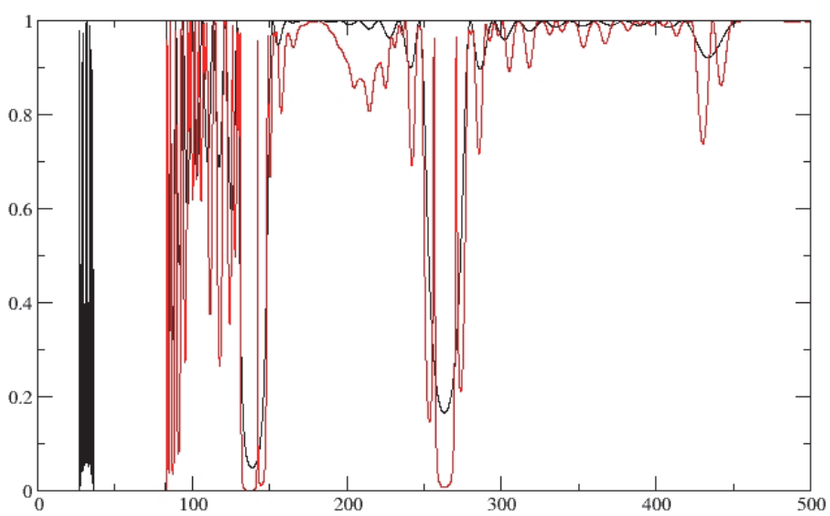

Fig. 15. Transmittance for an width/distance of 75Å, generation 10.

Once again using that $E'' \circ f_{a_N}^{-1} = \lambda_{a_N}^{-2}(E \circ f_{a_N}^{-1})''$ we get

$$(E \circ f_{a_N}^{-1})''(x) - \lambda_{a_N}^2 \alpha_{a_N}^2 \frac{\omega^2}{v(x)^2} E \circ f_{a_N}^{-1} = 0 \tag{30}$$

which implies that $E \circ f_{a_N}^{-1}$ is solution of the equation

$$Y''(x) - \frac{\tilde{\omega}^2}{v(x)^2} Y(x) = 0 \tag{31}$$

where $\tilde{\omega}^2 = \lambda_{a_N}^2 \alpha_{a_N}^2 \omega^2$, i. e., if we take the electric field for whole system E_T and we compares this with the corresponding to a rescaled copy $E_{\beta T}, \beta \in (0,1)$, then $\omega_{E_{\beta T}} = \lambda_{a_N} \alpha_{a_N} \omega_{E_T}$. This implies that $E_\omega(f_{a_N}^{-1}(x)) = E_{\omega'}(x)$.
Finally we consider the case in which $\lambda_{a_N} \alpha_{a_N} = 1$, in this case the electric field is self-similar in the space for a given energy, i. e. $E_\omega(f_{a_N}^{-1}(x)) = E_\omega(x)$.

5.2 Reflectance

For this case Lavrinenko et al (11) give an excellent analysis and presentation of this kind of systems. And the two main features that they distinguish are the scalability and the sequential splitting of the spectra.

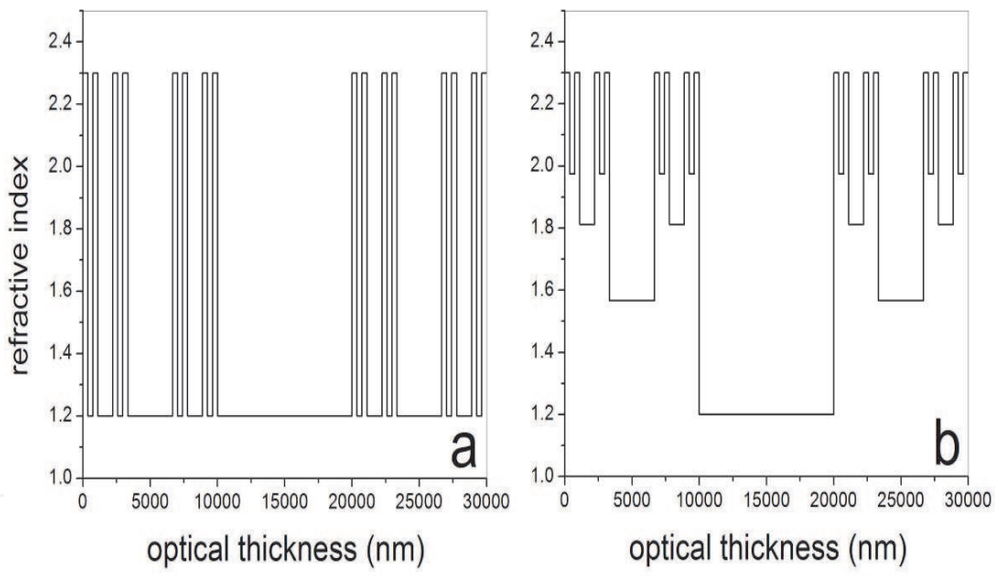

Fig. 16. Two types of fourth Cantor generation structures in which was applied the Cantor rule to a) the optical thickness and b) both the optical thickness as well as the refractive index.

According to the equation 31, it does not exist a limiting condition to find self-similar behavior of the electric field in the whole interval with respect to the restricted interval $f_{a_N}(I_0)$ of the system. So we generated two types of Cantor structures shown in figure 16 which satisfy the ternary Cantor rule. In the first case we applied the Cantor rule only to the optical thickness (nd) (type-I) while in the second case we applied it to the optical thickness as well as to the refractive index (type-II); both structures retain the same total optical thickness equal to 30 Îijm. Since the physical thickness is defined as the rate of the optical thickness divided by refractive index, the physical thickness of the second type Cantor structure is expected to be narrower than the first type in each generation.

Theoretical simulation of transmission spectra of the Cantor structures was performed using transfer formalism (29) (21), in which we assumed that the layers that constitute the Cantor structure are homogeneous, isotropic and infinite in two transverse directions. Figure 17 shows the results obtained for transmission spectra of different type-I Cantor generations. It can be observed that increasing the order of Cantor generation the transmission spectra becomes more complex, exhibiting very pronounced resonance peaks and shifts to short wavelengths due to a finest inner structure of Cantor multilayer, retaining the same total optical thickness in each generation. In order to compare the transmission spectra of each one, we normalize the spectra with respect to the smallest optical thickness (Λ_0) in each generation as shown in figure 18.

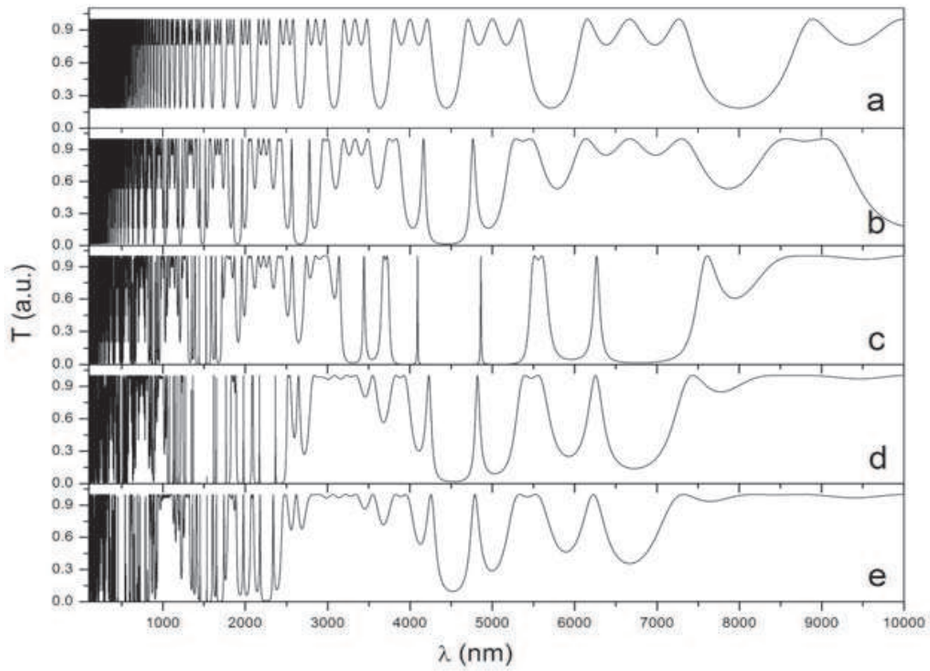

Fig. 17. Theoretical transmittance calculation of the type-I Cantor structures at different orders of generation: a) first, b) second, c) third, d) fourth and e) fifth. The calculation was realized using refractive indices of 2.3 and 1.2 remaining the same optical thickness equal to $30\mu m$ for all generations.

The normalized results display interesting optical properties of the Cantor structures. First, we observe that the transmittance spectra of the ith Cantor generation contains the previous $i-1$ Cantor generation. For example, the second Cantor generation spectra (Fig. 5.3 b) is present in each one of the following generations (Fig. 18 c, d y e, represented by the shadow area) which indicates that transmittance spectra exhibit self-similarity. Furthermore, the scaling factor required to scale the $i-1$ Cantor generation and reproduce the ith Cantor generation is the same used to scale the spatial thickness, i.e. equal to 3. These facts have been observed in other systems with high refractive index contrast (nB/nA=2.3)(11). However, the amplitude of the transmittance does not have a unique scale factor.

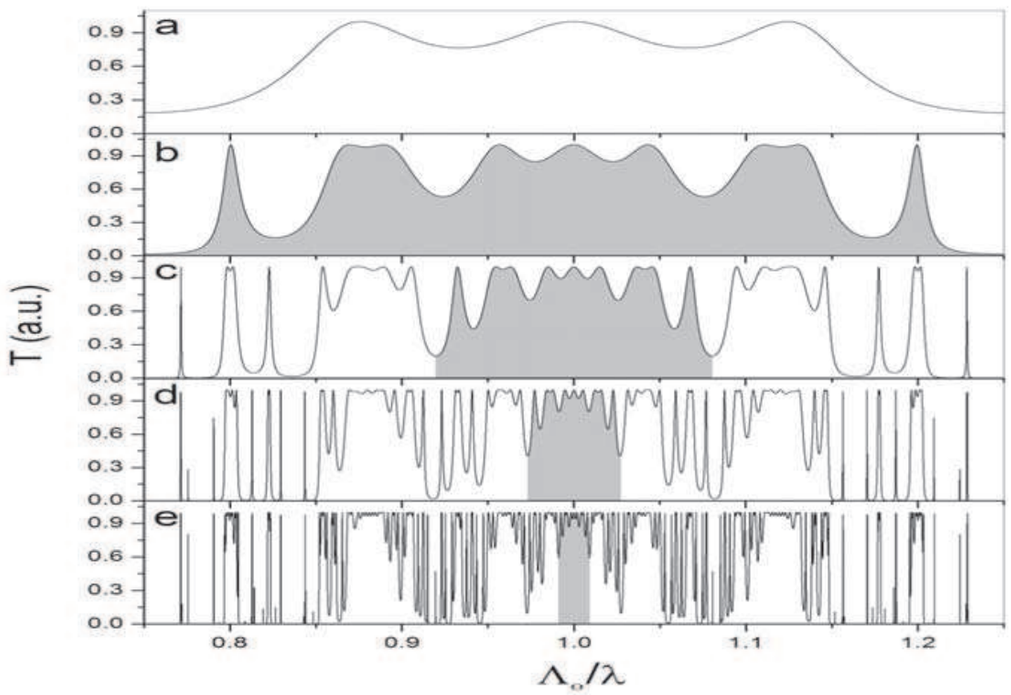

Fig. 18. Theoretical transmittance of the type-I Cantor structures normalized with respect to the optical thickness (Λ_0) of the smallest layer in each structure. The refractive indices and the whole optical thickness are the same used in the figure 17.

In figure 19 is shown the normalized transmittance spectra of the type-II Cantor structures for various Cantor generations. It is observed that the optical spectra are qualitatively similar to the obtained in type-I Cantor's. However, in this case, more transmission and reflection modes appear due to the multiple splitting of the optical thickness as well as the refractive index. Once more, the ith spectra is contained in the following generations and it is scaled by a factor of 3. But in this case it is possible to find a scaling factor to rescale the transmission amplitude of the $i+1$ Cantor spectra to reproduce the i Cantor spectra, and so on. This scaling factor was found to be approximately equal to 0.41.

5.2.1 Electric field

The distribution of electric field intensity along the structure for each type-I Cantor generation is shown in figure 20. The EF was calculated for a wavelength of 1650.70164 nm which corresponds to a very well defined transmission mode. Increasing the generation order, it follows that the intensity as well as the confinement of the electric field increases drastically reaching a maximum value of $|E|^2 = 477$ in the fourth generation. A subsequent increment the confinement of EF starts to decrease. Another interesting thing is the fact the confinement occur preferably in the central part of the Cantor structures and can be tuned to a particular wavelength by only scaling the whole Cantor structure, i.e. either increasing or reducing the total optical thickness. This can be exploited to the development of active nucleus in the heating, emitting and lasing applications such as LED's, lasers, etc.

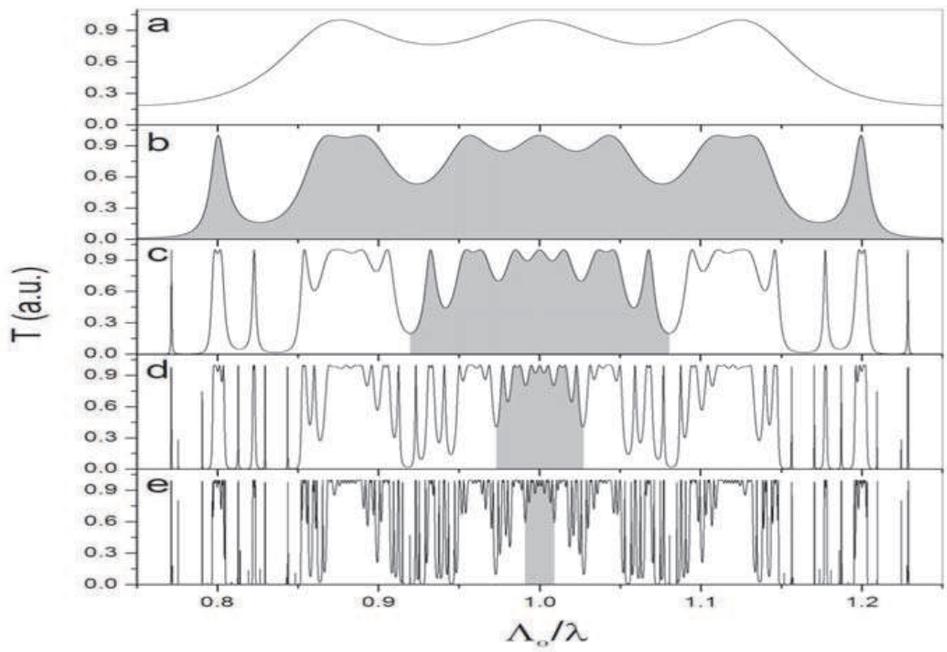

Fig. 19. Theoretical transmittance of the type-II Cantor structures normalized with respect to the optical thickness (Λ_0) of the smallest layer in each structure. The refractive indices and the whole optical thickness are the same used in the type-I Cantor structures.

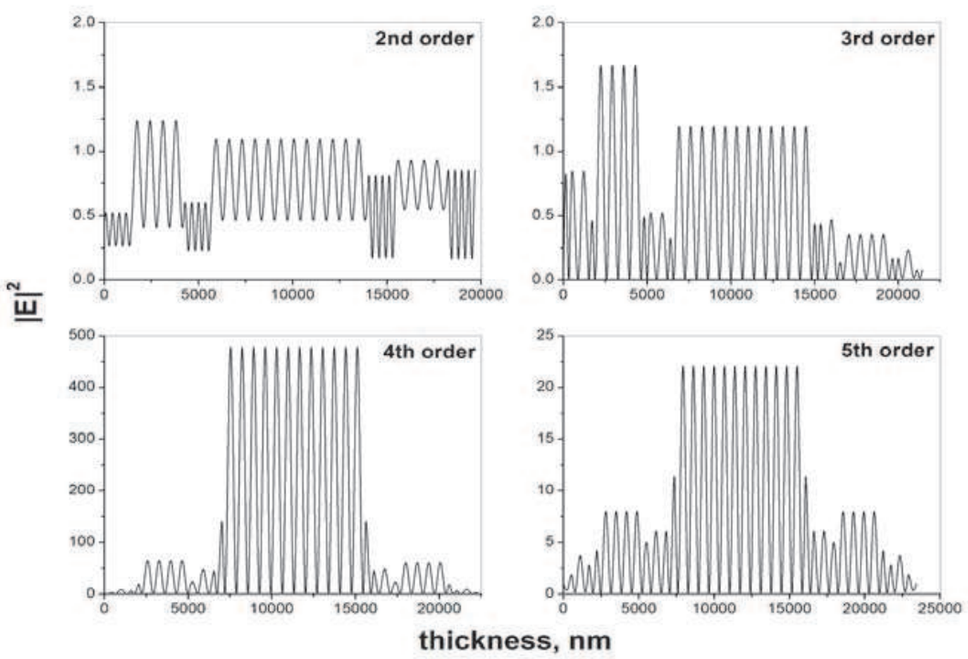

Fig. 20. Electric field intensity calculated at a wavelength of 1650.70164 nm for different type-I Cantor structures.

6. Conclusions

First, we have demonstrated that the wave functions exhibit a self-similar property induced by the *self-similarity* condition (9) on the potential. We have given a proof in the framework of quasiclassical approximation. This is true for energy values, no matter how large it could be. This behavior of the self-similar quantum well is radically different from that known from a standard quantum well, which only affects the eigenfunctions of the levels closest to the well top. On the other hand, we have observed some interesting properties for the discrete levels.
At first sight, it could be supposed that the system proposed is not different from those that appeared before in the literature. However, the system that we have considered are extremely different from a topological point of view, since the quantum well proposed is self-similar. This property, allows us to show that for any eigenvalues the associated eigenfunction “feels" the presence of the quantum well, despite how large is the eigenvalue. This is a main difference to the standard quantum well, where the eigenfunctions show the presence of the quantum well only for eigenvalues close to the well top.
At this stage of the study, it is more than likely acceptable to suggest that there are other bounded potentials defined in finite intervals also having self-similar wavefunctions. Indeed the standard Cantor construction can be changed in a variety of ways, as can be seen in Ref. (24), all of them having the same analytical properties. In a given Cantor construction one may study non-constant potentials, and the main steps of our analysis are valid as long as the *self-similar* condition (9) remains legitimate.
Other isomorphic problems possess the same properties. Among them we can mention the transversal horizontal elastic modes, the TE or TM electromagnetic modes, both of them in a multilayered system,(21) etc. It is not so evident, on the other hand, that non-isomorphic problems, like those discussed in Ref. (26), share the fractal property of the self-similarity of the corresponding states. But it is worth to mention that in quasiregular heterostructures, elementary excitations exhibit fractality as well as self-similarity of the zero state, despite being isomorphic with onedimensional Schrödinger-like equations.
The properties of the spectrum of different Hamiltonians is a problem of current interest for mathematicians as well as for physicists. A significant number of progresses have been obtained in the last decennials. As a survey the reader can be addressed to Refs. (1; 27; 28) and references therein. However, there remains a number of intriguing questions; one of them is the character of the spectrum for strange potentials as the one we have analyzed in this paper.
Apparently this strange potential could be described as nothing but a curiosity; however, this is not entirely true. In the present days the experimentalists can construct, and in fact they do, finite realizations of these bizarre systems obtaining interesting and applicative properties. We hope the present theoretical lucubration encourages some experimental works.
Furthermore, we have calculated the coefficient of intersubband optical absorption (in the region of the discrete spectrum of energies), but we have found no self-similarity, at least none evident.
We present a formal definition of topological self-similar potentials. These, not only have to show scaling properties in the length but also in the values of V. In this situation, the eigenfunctions of the discrete spectrum are self-similar by pairs. In this type of systems the eigenfunctions seems to be strongly localized at the small wells. This behavior suggest that the electronic mobility will be greater than the corresponding to traditional quantum wells.

On the other hand, the optical absorption coefficient does not present a remarkable behavior. The electronic transmittance for self-similar barriers shows certain interesting oscillations for high energies. Particularly interesting came to be the case of mixed systems. First, the ssp filters the tunneling transmittance of the mbpp. Also, it shows a gap in a permitted region of the corresponding mbpp. In this gap, it could be observed three quasibound levels. This behavior seems to be particular of these kind of mixing, as it can not be obtained with mbpp or multibarrier quasiregular potentials. The proof of theorem 2, shows that distinct types of selfsimilarity is obtained depending on the similar ratios that is taken for the construction of the potential.
The mixed systems modify the general behavior of the transmittance corresponding to the potential component systems. Also, the transmittance in function of the width of the barriers shows that the contribution of smaller barriers in the ssp is reflected on the whole structure of maximum and minimum. Finally, in the optical reflectance spectrum for a self-similar structure based on porous silicon, the more interesting property is the nesting from one generation to next. Which gives the possibility of characterize this kind of spectrum.

7. References

[1] J.M. Luck, *"Cantor spectra and scaling of gap widths in deterministic aperiodic systems"*, Phys. Rev. **B39**:9, 5834-5849 (1998).

[2] M. Kolár and F. Nori, *"Trace maps of general substitutional sequences"*, Phys. Rev. **B42**:1, 1062-1065 (1990).

[3] R. Pérez-Álvarez and F. García-Moliner, *"The spectrum of quasiregular heterostructures"*, invited chapter in "Some Contemporary Problems of Condensed Matter Physics", Nova Science Publishers, ed. by S. Vlaev and M. Gaggero-Sager (2000), pp. 1-37.

[4] E. Maciá and F. Domínguez, *"Phonons and Excitons in Low Dimensional Aperiodic Systems"*, Editorial Complutense, Madrid (2000).

[5] R. Pérez-Álvarez, F. García-Moliner, and V.R. Velasco *"Some elementary questions in the theory of quasiperiodic heterostructures"*, J. of Phys.: Condens. Matter **13**, 3689-3698 (2001).

[6] B.B. Mandelbrot, *"The Fractal Geometry of Nature"*, W.H. Freeman and Company, New York (1983).

[7] A. Bovier and J.M. Ghez, *"Spectral properties of one-dimensional Schrödinger operators with potentials generated by substitutions"*, Commun. Math. Phys. **158**:1, 45-66 (1993).

[8] A. Bovier and J.M. Ghez, *"Remarks on the spectral properties of tight-binding and Kronig-Penney models with substitution sequences"*, J. Phys. A:Math. Gen. **28**:8, 2313-2324 (1995).

[9] L.M. Gaggero-Sager, E.R. Pujals, and O. Sotolongo-Costa, *"Self-similarity in a Cantor-like semiconductor quantum well"*, Phys. Stat. Sol. (b) **220**, 167-169 (2000).

[10] S.V. Zhukovsky, A.V. Lavrinenko, and S.V. Gaponenko, *"Spectral scalability as a result of geometrical self-similarity in fractal multilayers"*, Europhys. Lett. **66**:3, 455-461 (2004).

[11] A.V. Lavrinenko, S.V. Zhukovsky, K.S. Sandomirski, and S. V. Gaponenko, *"Propagation of classical waves in nonperiodic media: Scaling properties of an optical Cantor filter"*, Phys. Rev. E **65**, 036621 (2002).

[12] L. Moretti, I. Rea, L. De Stefano, and I. Rendina, *"Periodic versus aperiodic: Enhancing the sensitivity of porous silicon based optical sensors"*, Applied Phys. Lett. **90**, 191112 (2007).

[13] V. Agarwal, B. Alvarado-Tenorio, Jose Escorcia-García, and Luis Manuel Gaggero-Sager, *"Cantor Dielectric Heterostructures Made of Nanostructured Multilayers of Porous Silicon"*, PIERS Online **4**:4, 451-454 (2008).
[14] Kenta Esaki, Masatoshi Sato, and Mahito Kohmoto *"Wave propagation through Cantor-set media: Chaos, scaling, and fractal structures"* Phys. Rev. E **79**, 056226 (2009)
[15] M. Pilevari Salmasi, F.H. Kahani, and M.N. Azarmanesh, *"A novel broadband fractal Sierpinski shaped, microstrip antenna"*, Progress In Electromagnetics Research C **4**, 179-190 (2008).
[16] Massimiliano Berti and Philippe Bolle, *"Cantor families of periodic solutions for completely resonant wave equations"*, Frontiers of Mathematics in China, **3**:2, 151-165 (2008).
[17] Artur Avila, Jairo Bochi, and David Damanik, *"Cantor spectrum for Schrödinger operators with potentials arising from generalized skew-shifts"*, Duke Math. J. **146**:2, 253-280 (2008).
[18] J.Palis and F.Takens *Hyperbolicity and sensitive-chaotic dynamics at homoclinic bifurcations* Cambridge University Press, 1993.
[19] C. G. Moreira, J-C. Yoccoz, Stable intersections of regular Cantor sets with large Hausdorff dimensions. *Ann. of Math. (2)* **154** (2001), no. 1, 45-96.
[20] L.D. Landau and E.M. Lifschitz, *"Mecanique Quantique"*, éditions Mir, Moscou (1966).
"Quantum Mechanics, Nonrelativistic theory", Pergamon, New York (1981).
"Mecánica Cuántica (teoría no-relativista)", editorial Reverté S.A. Barcelona-Buenos Aires-Mexico (1967).
[21] D.J. Griffiths and C.A. Steinke, *"Waves in locally periodic media"*, Am. J. Phys. **69**:2, 137-154 (2001).
[22] G. Bastard, *"Wave mechanics applied to semiconductor heterostructures"*, Éditions de Physique, Paris (1989).
[23] S.N. Rasband, *"Chaos dynamics of nonlinear systems"*, Wiley Professional Paperback Series (1997).
[24] T.C. Halsey, M.H. Jensen, L.P. Kadanoff, I. Procaccia, and B.I. Shraiman, *"Fractal measures and their singularities: The characterization of strange sets"*, Phys. Rev. **A33**:2, 1141-1151 (1986).
[25] S.Ya. Jitomirskaya and Y. Last, *"Dimensional Hausdorff properties of singular continuous spectra"*, Phys. Rev. Lett. **76**:11, 1765-1769 (1996).
[26] R. Pérez-Álvarez, F. García-Moliner, C. Trallero-Giner, and VR Velasco, *"Polar optical modes in Fibonacci heterostructures"*, Journal of Raman Spectroscopy **31**:5, 421-425 (2000).
[27] B. Simon, *"Almost periodic Schrödinger operators: A review"*, Adv. Appl. Math. **3**, 463-490 (1982).
[28] B. Simon, *"Schrödinger operators in the twenty-first century"*, eds. A. Fokas, A. Grigoryan, T. Kibble, and B. Zegarlinski, Imperial College, London, 283-288 (2000). Also at J. Math. Phys. **41**, 3523-3555 (2000).
[29] M. E. Mora, R. Pérez-Álvarez and C. Sommers, J. Physique **46**, 1021-1026 (1985).

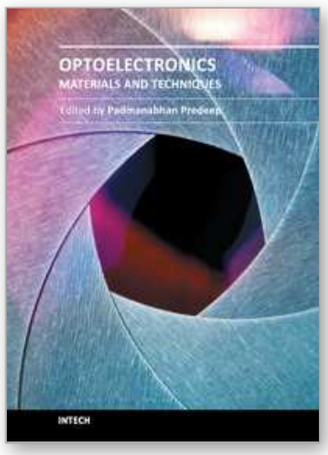

Optoelectronics - Materials and Techniques

Edited by Prof. P. Predeep

ISBN 978-953-307-276-0
Hard cover, 484 pages
Publisher InTech
Published online 26, September, 2011
Published in print edition September, 2011

Optoelectronics - Materials and Techniques is the first part of an edited anthology on the multifaceted areas of optoelectronics by a selected group of authors including promising novices to the experts in the field. Photonics and optoelectronics are making an impact multiple times the semiconductor revolution made on the quality of our life. In telecommunication, entertainment devices, computational techniques, clean energy harvesting, medical instrumentation, materials and device characterization and scores of other areas of R&D the science of optics and electronics get coupled by fine technology advances to make incredibly large strides. The technology of light has advanced to a stage where disciplines sans boundaries are finding it indispensable. Smart materials and devices are fast emerging and being tested and applications developed in an unimaginable pace and speed. Here has been made an attempt to capture some of the materials and techniques and underlying physical and technical phenomena that make such developments possible through some real time players in the field contributing their work and this is sure to make this collection of essays extremely useful to students and other stake holders such as researchers and materials scientists in the area of optoelectronics.

INTECH
open science | open minds

InTech Europe
University Campus STeP Ri
Slavka Krautzeka 83/A
51000 Rijeka, Croatia
Phone: +385 (51) 770 447
Fax: +385 (51) 686 166
www.intechopen.com

InTech China
Unit 405, Office Block, Hotel Equatorial Shanghai
No.65, Yan An Road (West), Shanghai, 200040, China
中国上海市延安西路65号上海国际贵都大饭店办公楼405单元
Phone: +86-21-62489820
Fax: +86-21-62489821

IntechOpen